BRAIN
ORIGINAL ARTICLE

Distinct signatures of loss of consciousness in focal impaired awareness versus tonic-clonic seizures

Elsa Juan,[1,2,†] Urszula Górska,[1,3,†] Csaba Kozma,[1,4,†] Cynthia Papantonatos,[4] Tom Bugnon,[1] Colin Denis,[4] Vaclav Kremen,[5,6] Greg Worrell,[5] Aaron F. Struck,[4,7] Lisa M. Bateman,[8] Edward M. Merricks,[9] Hal Blumenfeld,[10] Giulio Tononi,[1] Catherine Schevon[9] and Melanie Boly[1,4]

[†]These authors contributed equally to this work.

Loss of consciousness is a hallmark of many epileptic seizures and carries risks of serious injury and sudden death. While cortical sleep-like activities accompany loss of consciousness during focal impaired awareness seizures, the mechanisms of loss of consciousness during focal to bilateral tonic-clonic seizures remain unclear. Quantifying differences in markers of cortical activation and ictal recruitment between focal impaired awareness and focal to bilateral tonic-clonic seizures may also help us to understand their different consequences for clinical outcomes and to optimize neuromodulation therapies.

We quantified clinical signs of loss of consciousness and intracranial EEG activity during 129 focal impaired awareness and 50 focal to bilateral tonic-clonic from 41 patients. We characterized intracranial EEG changes both in the seizure onset zone and in areas remote from the seizure onset zone with a total of 3386 electrodes distributed across brain areas. First, we compared the dynamics of intracranial EEG sleep-like activities: slow-wave activity (1–4 Hz) and beta/delta ratio (a validated marker of cortical activation) during focal impaired awareness versus focal to bilateral tonic-clonic. Second, we quantified differences between focal to bilateral tonic-clonic and focal impaired awareness for a marker validated to detect ictal cross-frequency coupling: phase-locked high gamma (high-gamma phased-locked to low frequencies) and a marker of ictal recruitment: the epileptogenicity index. Third, we assessed changes in intracranial EEG activity preceding and accompanying behavioural generalization onset and their correlation with electromyogram channels. In addition, we analysed human cortical multi-unit activity recorded with Utah arrays during three focal to bilateral tonic-clonic seizures.

Compared to focal impaired awareness, focal to bilateral tonic-clonic seizures were characterized by deeper loss of consciousness, even before generalization occurred. Unlike during focal impaired awareness, early loss of consciousness before generalization was accompanied by paradoxical decreases in slow-wave activity and by increases in high-gamma activity in parieto-occipital and temporal cortex. After generalization, when all patients displayed loss of consciousness, stronger increases in slow-wave activity were observed in parieto-occipital cortex, while more widespread increases in cortical activation (beta/delta ratio), ictal cross-frequency coupling (phase-locked high gamma) and ictal recruitment (epileptogenicity index). Behavioural generalization coincided with a whole-brain increase in high-gamma activity, which was especially synchronous in deep sources and could not be explained by EMG. Similarly, multi-unit activity analysis of focal to bilateral tonic-clonic revealed sustained increases in cortical firing rates during and after generalization onset in areas remote from the seizure onset zone.

Overall, these results indicate that unlike during focal impaired awareness, the neural signatures of loss of consciousness during focal to bilateral tonic-clonic consist of paradoxical increases in cortical activation and neuronal firing

Received October 6, 2021. Revised May 17, 2022. Accepted June 11, 2022. Advance access publication November 16, 2022

found most consistently in posterior brain regions. These findings suggest differences in the mechanisms of ictal loss of consciousness between focal impaired awareness and focal to bilateral tonic-clonic and may account for the more negative prognostic consequences of focal to bilateral tonic-clonic.

1 Department of Psychiatry, University of Wisconsin-Madison, Madison, WI 53719, USA
2 Department of Psychology, University of Amsterdam, Amsterdam, 1018 WS, The Netherlands
3 Smoluchowski Institute of Physics, Jagiellonian University, 30-348 Krakow, Poland
4 Department of Neurology, University of Wisconsin-Madison, Madison, WI 53705, USA
5 Department of Neurology, Mayo Clinic, Rochester, MN 55905, USA
6 Czech Institute of Informatics, Robotics, and Cybernetics, Czech Technical University in Prague, Prague, 16000, Czech Republic
7 Department of Neurology, William S. Middleton Veterans Administration Hospital, Madison, WI 53705, USA
8 Department of Neurology, Cedars-Sinai Medical Center, Los Angeles, CA 90048, USA
9 Department of Neurology, Columbia University, New York City, NY 10032, USA
10 Department of Neurology, Yale School of Medicine, New Haven, CT 06519, USA

Correspondence to: Melanie Boly
Department of Neurology
600 Highland Avenue, Madison WI 53792, USA
E-mail: boly@neurology.wisc.edu

Keywords: ictal rhythms; epileptic seizures; generalization; consciousness; responsiveness

Introduction

Epilepsy is a frequent and disabling disease. In the USA, 5% of the population will have at least one seizure in their lifetime, while chronic epilepsy affects ~3 million adults and 470 000 children.[1] About one-third of chronic epilepsies are refractory to pharmacological treatment,[2] and surgery to achieve seizure freedom can only be performed in a minority of these cases.[3] Seizures that are accompanied by loss of consciousness (LOC) have especially detrimental consequences on quality of life, partly through their impact on driving limitations and on social stigmatization.[4,5] Among all seizure types, focal to bilateral tonic-clonic (FBTC; previously called 'secondarily generalized') seizures are the most disabling, due to a complete inability to control behaviour and an increased risk of sudden death.[6–8] Although focal impaired awareness (FIA; previously called 'complex partial') seizures can also lead to serious injuries—for example if they occur while driving—they are usually characterized by a partial impairment of responsiveness.[9,10] Unlike FBTC, a partial recall of subjective experiences is often observed after FIA.[11,12] Importantly, frequent FBTC also predicts poorer cognitive and surgical outcomes compared to frequent FIA.[13]

In recent years, direct intracranial EEG (iEEG) studies in humans showed that during FIA of temporal lobe onset, sleep-like slow-wave activity (SWA; 1–4 Hz) is seen in widespread bilateral cortical networks, while ictal activity itself is restricted to a small area surrounding the seizure onset zone (SOZ).[14] This discovery led to the development of promising neuromodulation therapies targeting arousal centres to reverse LOC during FIA.[15,16] While it was reported that FIA and FBTC share similar electrographic ictal onset patterns,[17] the electrophysiological correlates of behavioural generalization and LOC during FBTC have not yet been quantified. A better understanding of the cortical dynamics driving the evolution of focal seizures towards generalization could have broad implications for preventive approaches to FBTC.

Previous studies suggested that ictal activity is limited to a small cortical area during FIA.[14] However, the occurrence of high-frequency oscillations (HFO, >80 Hz) beyond SOZ was reported during FIA in other studies.[18] While increased HFO has also been reported during FBTC,[19] previous studies in small samples suggested that they may not invade the whole cortex.[17,20,21] Importantly, increased HFO do not per se signal ictal recruitment; they can increase during deep non-REM sleep[22] and in the ictal penumbra (cortical areas that are not actively seizing).[23] Recently, delayed-onset ictal high-gamma activity (80–150 Hz) phase-locked to lower frequencies (4–30 Hz) ('phase-locked high gamma', PLHG)[18] has been shown to constitute a reliable proxy for synchronized multi-unit firing bursts in the actively seizing cortex (ictal core).[24,25] PLHG applied to clinical iEEG recordings[26] has also been shown to predict surgical outcomes—the current gold standard to assess localization accuracy for the epileptogenic zone—more accurately than HFOs alone.[18,27] Thus, we here sought to quantify differences in ictal cross-frequency coupling between FIA and FBTC using PLHG. As a marker of spatial ictal recruitment, we also compared the number of channels passing a threshold of energy ratio (ER) between high and low frequencies—which forms the basis of the computation of the epileptogenicity index (EI)[28]—between FIA and FBTC. The EI detects the ordering through which each channel crosses the threshold for ictal recruitment to define the SOZ; it can successfully predict surgical outcome.[29]

Here we aimed to address four main points: (i) whether LOC during FBTC (as compared to FIA) is accompanied by sleep-like activities; (ii) whether ictal recruitment is widespread during FBTC; (iii) what the iEEG signatures of behavioural generalization are; and (iv) how neuronal firing changes during FBTC in areas remote from the SOZ.

By comparing the temporal and spatial evolution of iEEG sleep-like activities and ictal rhythms in FBTC and FIA across 179 seizures from several academic centres, our results provide new insights about the electrocortical and neuronal firing patterns involved in secondary generalization and suggest different mechanisms for LOC during FBTC compared to FIA. The current results may have implications to understand mechanisms of LOC and differences

in clinical outcomes and could have implication for preventive treatments and neuromodulation strategies.

Material and methods

Datasets

Seizures were retrospectively collected from University of Wisconsin-Madison (UW-Madison) Hospital and Clinics (UWHC) medical records, from the iEEG.org online database,[30] and from the European Epilepsy Database (EED[31]). Only seizures acquired at 400 Hz sampling rate or higher, with good quality iEEG recording, with pre- and post-electrode implantation CT and MRI scans (or that included electrodes' MNI coordinates) and with a reliable seizure type scoring (FBTC versus FIA) were considered. A total of 179 seizures (50 FBTC, 129 FIA) from 41 epilepsy patients (19 female, median age 33 years old, range 14–63) implanted with intracranial electrodes were eventually included: 55 seizures from UWHC, 34 seizures from iEEG.org (mostly from the Mayo Clinic) and 90 seizures from the EED. The number of seizures per patient was lower for FBTC than for FIA (resp. 1.1 ± 1.5 and 3 ± 3.8; $t(178) = 2$, $P = 0.006$; see Table 1). Most seizures originated from the temporal lobe (80% FBTC and 87% FIA; $P = 0.3$ Fisher; see Table 1 for a comprehensive breakdown). Most seizures originated from the left hemisphere, but this was more often the case for FBTC than for FIA (57% of the FIA and 76% of the FBTC; $P = 0.02$ Fisher). A comparable number of seizures arose from sleep in both seizure types (see Table 1). Considering electrographic onset patterns, most FBTC originated from rhythmic activity (48% of FBTC), while FIA often arose from low amplitude fast activity (LAFA; 40% of FIA); spiking activity was the least common onset pattern in both seizure type (20% of FBTC, 23% of FIA). No differences in electrographic onset pattern were found between FBTC and FIA ($P = 0.4$, $\chi^2 = 2.04$). Stereo-EEG (SEEG) and subdural grids and depth electrodes (SGDE) were used to a similar extent in FIA and FBTC (see Table 1). FBTC lasted on average 121 ± 77 s and FIA 107 ± 69 s [$t(178) = -1.23$, $P = 0.2$].

Three additional FBTC from Columbia University from two patients with left temporal focus (two males, 28 and 29 years old) containing both iEEG and Utah microelectrode array recordings were included for firing rate analysis. All procedures were approved by the institutional review board for human studies at the University of Wisconsin-Madison and at Columbia University. Informed consent was collected for the two patients prospectively enrolled at Colombia University.

Table 1 Patient's clinical characteristics split by seizure type

	FBTC	FIA	P value (t value)
Patients, *n*	20[a]	32[a]	–
Seizures, *n*	50	129	–
Seizures per patient, *n*	1.1 ± 1.5	3 ± 3.8	**0.006 (2)**
Seizure duration, s	121 ± 77	107 ± 69	0.2 (–1.23)
Primary seizure focus, *n* (%)			
Temporal	40 (80)	112 (87)	0.3 (Fisher)[b]
Frontal	5 (10)	16 (12)	
Parieto-occipital	5 (10)	1 (1)	
Left hemisphere onset, *n* (%)	38 (76)	73 (57)	**0.02 (Fisher)**
Electrographic onset pattern, *n* LAFA/rhythmic/spiking	16/24/10	52/47/30	0.4 ($\chi^2 = 2.04$)
Seizure arising from sleep, *n* (%)	25 (50)	49 (38)	0.2 (Fisher)
SEEG contacts per seizure, *n* (*n* seizures)	32 [8–126] (37)	25 [4–130] (110)	0.7 (0.4)
SGDE contacts per seizure, *n* (*n* seizures)	72 [18–100] (36)	52 [16–104] (95)	0.8 (0.2)
Abnormal MRI findings, *n* (%)	34 (68)	89 (69)	1 (Fisher)

Percentages are calculated relative to the total number of seizures of each type. Seizures per patient and seizure duration values are expressed as mean ± standard deviation. Electrode contacts per seizure are expressed as median [range]. Bold text indicates significant values ($P < 0.05$).
LAFA = low amplitude fast activity; SEEG = stereo-EEG; SGDE = subdural grid and standard depth electrodes.
[a]Nine patients had both FBTC and FIA seizures and two patients were recorded twice.
[b]Comparing seizures of temporal versus extra-temporal origin.

Electrographic timing, seizure categorization and behavioural scoring

The timing of seizure onset and offset was determined electrographically by a certified epileptologist (M.B.) for each seizure. Seizure onset time was established at the first sign of epileptic activity (e.g. heralding spike) on any channel. Seizure offset time was established when epileptic activity had ceased on all channels. The SOZ was determined on the basis of the first channels to show epileptiform activity.

Seizure classification was determined on the basis of behavioural manifestations occurring in the ictal period. According to the 2017 ILAE guidelines,[32] we categorized seizures as FIA when response to commands or to questions was impaired or when there was amnesia at any point during the seizure (as in Englot *et al.*[14]). FBTC seizures were recognized on the basis of the additional occurrence of symmetric or asymmetric bilateral stiffening (tonic phase) followed by bilateral convulsions (clonic phase). We considered the start of the tonic phase as the onset of behavioural generalization.

When simultaneous audio and video recordings were available (e.g. in UWHC, iEEG.org and Columbia datasets), the timing of behavioural manifestations in relation to the iEEG signal was also recorded. Two main dimensions were considered: ability to follow simple commands (with scores split between verbal responsiveness and motor responsiveness), and amnesia.[14] We also classified patient's behaviour on some of the dimensions of the Consciousness in Seizures Scale (CSS)[33] that could be consistently assessed: whether the patient was able to interact with an examiner (CSS 3), and whether the patient was aware of having a seizure while it occurred (CSS 4). Behaviour was further quantified separately for the first and second half of FIA, and for the pre-generalization and the post-generalization periods of FBTC. A subset of six FBTCs for which the duration of the pre-generalization phase exceeded 60 s was also analysed behaviourally. The pre-generalization phase was split in two halves (consistent with ~30 s original temporal resolution of the behavioural analysis). Considering that two seizures had to be excluded (behaviour could not be reliably characterized in the first half of the pre-generalization phase), the final analysis counted four FBTC linking behaviour and brain activity during ~30 s earlier versus ~30 s later parts of pre-generalization phase. For seizures without video recordings (e.g. all EED seizures and some iEEG.org seizures), we relied on information provided by the database for seizure classification. These seizures were not included in analyses focusing on the temporal evolution of LOC.

Intracranial data preprocessing

Electrode localization was done semi-automatically using the iElectrodes toolbox[34] and the FMRIB Software Library (FSL[35]). The post-implantation CT scan was aligned to the pre-implantation MRI and registered to standard MNI space. Corresponding electrodes' voxels were then manually selected, automatically clustered and accordingly labelled [Fig. 1 A(i)–A(iii)]. On the basis of the MNI coordinates identified for each electrode, probabilistic assignment to brain regions were obtained using the Talairach client.[36,37] Contacts were then grouped in temporal, frontal and parieto-occipital areas. Following the Lundstrom *et al.*[38] approach, electrodes within a 2.5 cm distance from the clinically identified SOZ were further separated from other electrodes and grouped as an SOZ area. It is important to note that although most seizures originated from the temporal lobe, some seizures were of extra-temporal origin; therefore, SOZ electrodes include extra-temporal locations.

All iEEG data were acquired using either a subgaleal electrode (for SGDE) or a scalp electrode (for SEEG) as reference. This scalp electrode was placed in a fronto-central position (i.e. between Cz and Fz) for iEEG.org and EED, and to the right or left mastoid for UWHC. IEEG signal was preprocessed with customized scripts using routines from the EEGLAB toolbox version 14.1[39] running on MATLAB 2016b (Mathworks Inc., Natick, MA, USA). A baseline consisting of minimum of 2 min (maximum 5 min) of pre-ictal iEEG signal was included (see Fig. 1 B1–B2 for exemplar FIA and FBTC seizures). The raw signal was down-sampled to 400 Hz (including anti-aliasing filter) and bandpass filtered ~0.5–199 Hz using Hamming windowed sinc Finite Impulse Response (FIR) filter. Line noise was removed when appropriate using the CleanLine algorithm (part of EEGLAB) on selected frequencies (mostly 60, 120 and 180 Hz). Channels and epochs with important artefacts (e.g. muscle activity) were rejected on the basis of visual inspection.

Power spectrum analyses and considered time periods

Power spectrum density was calculated for each contact using the 'pwelch' function with a 10 s window with 1 s overlapping window. Power spectrum values were then averaged over frequency bands of interest: SWA (1–4 Hz), beta (15–25 Hz) and high gamma (HG; 80–150 Hz). In addition, the beta/delta ratio (B/D) was calculated as the quotient of beta power over SWA power.

SWA was used as a marker of sleep-like activities, as previously shown during FIA.[14] Because B/D has been shown to differentiate sleep from wakefulness better than SWA within iEEG recordings,[40,41] we considered B/D to be an indicator of cortical activation. Considering that 80–150 Hz HG synchrony more specifically increases in actively seizing areas,[42,43] we used this range of HG activity to quantify ictal activation.

Finally, we computed phase-locked HG (PLHG; i.e. HG phased-locked to low 4–30 Hz oscillations) to obtain a marker of ictal activation validated to selectively increase in recruited areas.[18] For each electrode, we obtained instantaneous phase and amplitude for high- and low-frequency components from the Hilbert transform of the respectively high- (80–150 Hz) and low-pass (4–30 Hz) filtered signals (windowed sinc FIR filter with Hamming window). The PLHG index was then computed within non-overlapping 1 s sliding windows as:

$$PLHG = \frac{1}{N}\left|\sum_{n=1}^{N} a_{\mathrm{norm}(80-150\,\mathrm{Hz})}[n]\exp\left(i\left(\phi_{4-30\,\mathrm{Hz}}[n] - \phi_{a(80-150\,\mathrm{Hz})}[n]\right)\right)\right| \quad (1)$$

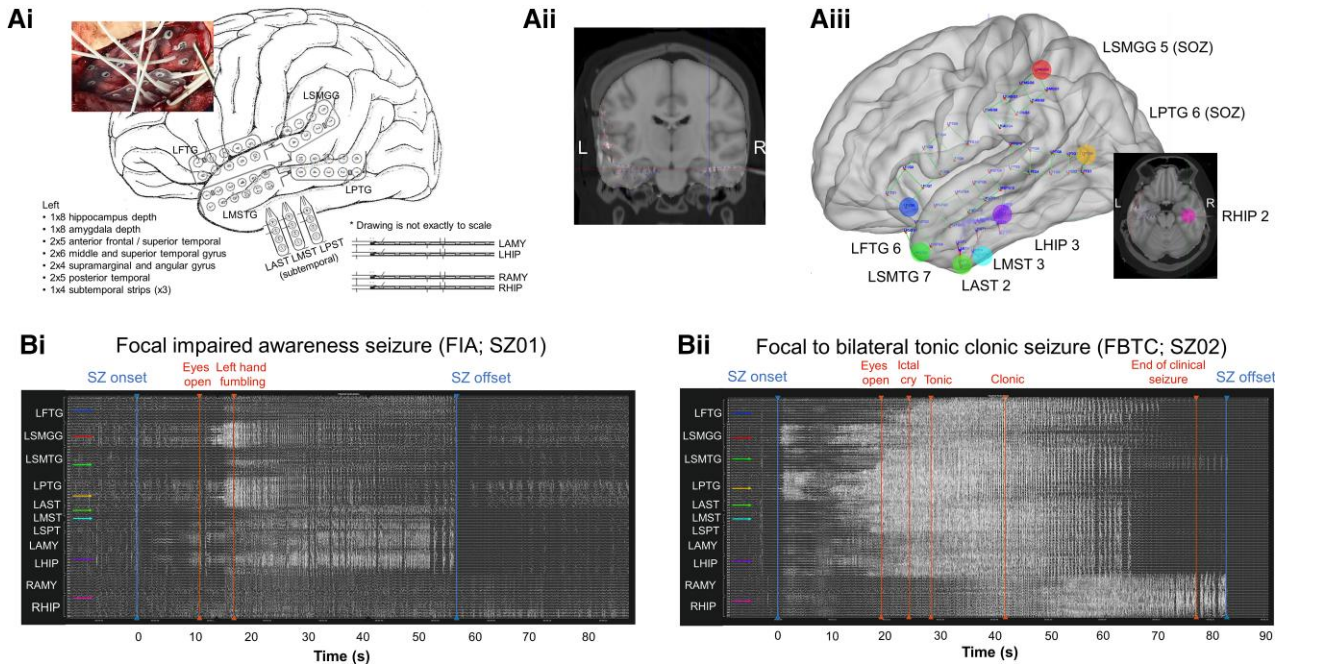

Figure 1 Exemplar 3D localization of intracranial electrodes and iEEG signal for one FIA and one FBTC seizure originating from a representative patient. (**A**) The surgical implantation and clinical electrode map (**i**) are used to locate electrodes positions in the post-implantation CT and pre-implantation MRI images, aligned in MNI standard space using the iElectrodes software (**ii**); eventually, final electrodes localizations are displayed on a standard MRI template (**iii**). (**B**) Time courses of raw iEEG signals for (**i**) one FIA and (**ii**) one FBTC seizure, along with marked behavioural events. Arrows indicate electrodes, with the locations specified with filled circles in [**A(iii)**]. Contacts LSMGG 5 and LPTG 6 were identified as belonging to the SOZ.

where N is the number of samples within the window, $a_{norm(80–150\ Hz)}$ is the instantaneous HG amplitude normalized by the average HG amplitude during baseline, $\phi_{4–30\ Hz}$ is the phase of the low-frequency component and $\phi_{a(80–150\ Hz)}$ is the instantaneous phase obtained from a second Hilbert transform applied to instantaneous HG amplitudes.[18,44]

To characterize the temporal evolution of different EEG features during seizures, the ictal period was split in two equal parts: the 'first seizure half' corresponding to the seizure onset up to the midpoint of the seizure, and the 'second seizure half' corresponding to the midpoint to the ictal offset. FBTC seizures were also divided in two epochs based on the time of generalization. Note that a separate analysis described next looked at EEG correlates of behavioural generalization itself. Ictal values were normalized by pre-ictal baseline values for each seizure separately.

We performed group statistics using a linear mixed-effect (LME) model on normalized power values, with separate models fitting for each previously mentioned frequency band. Patient and seizure were entered as random effects, and seizure type, brain region and ictal period as fixed effects. The use of restricted maximum likelihood estimates of the LME parameters allowed to account for the lack of independence between subjects and between seizures inherent to this dataset. The assumptions of the model were satisfied as the residuals showed Gaussian distribution. Statistical significance was evaluated at level $P < 0.001$ and corrected for multiple comparisons using false discovery rate (FDR[45]). All analyses were performed in R (R Core Team, 2015), using the lme4 package.[46]

Epileptogenicity index and SWA synchrony

To detect the spread of ictal recruitment, we quantified the number of channels crossing the ER threshold between high and low frequencies used to compute the epileptogenicity index (EI).[28] The EI is a validated measure of difference in timing of ictal recruitment between intracranial channels. It is typically used to determine the most likely SOZ by ranking channels according to the delay of their ictal involvement. We used ER threshold crossing to compute a proxy of the number of recruited channels during each seizure and compare the proportion of recruited channels across the whole brain and in each brain region between FIA versus FBTC.

We also used timing information of ER threshold crossing to compare the (a)synchrony in ictal onset across iEEG channels during FIA versus FBTC. Specifically, we defined the asynchrony parameter for a given seizure as the proportion of channels for which between-channels time difference of ictal recruitment (assessed with ER) was larger than 1 s versus the total number of channels or active channels (ratio in Supplementary Table 5). In doing so, we aimed to capture the relative number of clusters of channels activating >1 s apart from other channels or group of channels. As another marker of (a)synchrony, we quantified differences in the timing of peaks in SWA power (window size of 10 s and windows step of 1 s), and of HG power (same parameters) for comparison. For each seizure, we assessed the proportion of channels for which between-channels time difference of SWA peak power was >1 s apart versus all active channels. Finally, we also computed differences in timing of the peak amplitude of slow waves (SWs). SWs were detected within each channel using the procedure described by[47] (1–4 Hz bandpass, third-order Chebyshev filter). We then assessed averaged SWs amplitude using sliding windows with window size of 10 s and windows step of 1 s and marked the position in time with maximal negative peak for each channel. For each seizure, we then calculated the proportion of channels for which the between-channels time difference of negative peak was at least 1 s versus all active channels. We then computed group statistics for those measures of SWA asynchrony to compare FIA and FBTC (Supplementary Table 5).

Characterize the iEEG signatures of behavioural generalization

To characterize the electrographic changes accompanying generalization, we quantified iEEG brain activity changes preceding and coinciding with the onset of bilateral tonic phase. We selected a subset of 25 FBTC for which the onset of behavioural generalization (i.e. the start of the tonic phase) was known (from both UWHC and iEEG.org), and split the ictal period in pre- or post-generalization periods. We also analysed 20/25 FBTC seizures where behavioural data clearly pointed to either full LOC (16/20) versus fully preserved consciousness (4/20) at seizure onset. Because these four FBTC seizures also happened to have a prolonged pre-generalization phase, we could further split their pre-generalization period into two halves (preserving a temporal resolution of ~30 s for behavioural analysis as used in FIA and other FBTC). To differentiate the markers of generalization versus seizure onset, we contrasted SWA, B/D, HG and PLHG indices during the pre-ictal period, the pre-generalization period and the post-generalization periods.

To assess which iEEG indices were predictive of evolution of a seizure towards generalization, we compared SWA, B/D, HG and PLHG indices between the pre-generalization phase of FBTC and the first half of a subset of 57 FIA (coming from the same source as FBTC). The FBTC pre-generalization period lasted on average 26 ± 43 s and FIA first half 39 ± 51 s (median $\pm$ IQR), resulting in similar durations ($U = 837$, $P = 0.2$).

Although our analysis included exclusively iEEG signals from intracranial sources—thus limiting the contribution of muscle artefacts to high-frequency activity—we further wished to ensure that our results were not contaminated by extra-cerebral signals such as EMG activity.[48–50] To investigate this point, we computed the contribution of EMG signals to iEEG channels filtered in HG band using linear regression in five FBTC recordings (including depth and surface iEEG channels from both left and right hemispheres) where EMG data was available (two from UWHC, three from the EED). Because time-resolved behavioural data were not available in FBTC coming from EED, a proxy of generalization time was defined using timing of changes in HG. We first validated this measure in all 25 FBTC seizures for which behaviour timing was available by calculating the average delay between the highest slope of increase in HG power and the behavioural generalization timepoint. On average, behavioural generalization occurred 10.93 ± 5.98 s (mean $\pm$ SEM) after HG highest increase slope (see Fig. 5C). To take into account global differences in amplitude, linear regression was preferred over bipolar contact subtraction, however bipolar montages between EMG and EEG led to similar results. We computed EEG/EMG synchrony for the whole ictal period and reported results separately for the pre-ictal, the pre-generalization and the post-generalization periods.

To examine the possible contribution of intra- versus extracranial sources and the possible presence of a subcortical third driver, we also computed the contribution of deep versus superficial iEEG signals in the HG band using linear regression. We included 17 FBTC for which both deep and superficial contacts were available (seven FBTC from UWHC, one FBTC from iEEG.org and nine FBTC from EED). In particular, we contrasted changes in synchrony in

deep (amygdala/hippocampus) versus superficial (neocortical) iEEG contacts between pre- and post-generalization periods. Deep and superficial iEEG contacts were normalized by their distance to avoid any bias on synchrony that could be attributed to different distance between contacts. The previously mentioned proxy for generalization time was applied for FBTC for which the point of behavioural generalization was unknown.

Quantification of neuronal firing rates

To assess whether high-frequency power changes at the macro level in intracranial recordings of FBTC could indicate micro level changes in neuronal firing, we used a unique dataset combining macro- and microelectrode recordings. We analysed three additional FBTC seizures recorded in human epileptic subjects, where both iEEG and multi-unit activity were recorded, with Utah arrays located in areas remote from the SOZ (in the ictal penumbra, not recruited by the focal ictal process). We quantified local increases in firing rates compared to baseline, and their correspondence to sustained HG increases and behavioural generalization during FBTC.

Spike waveforms were detected on 30 kHz signal, filtered using a 1024th order FIR bandpass filter from 300 to 5000 Hz, using a detection threshold of 4.5σ, where $\sigma = \text{median}\left(\frac{|signal|}{0.6745}\right)$ estimates the standard deviation of the background noise.[51]

From here, spike waveforms from the peri-ictal and ictal periods were examined separately, since traditional spike sorting methods have been shown to fail in ictal recordings.[52] Waveforms from the peri-ictal period were sorted visually after *k*-means clustering using the UltraMegaSort2000 MATLAB toolbox,[53] and noise artefacts were removed. Ictal unit firing was then analysed using methods of Merricks *et al.*[54] Spike waveforms from the ictal period were template-matched to sorted peri-ictal putative units if the principal component vector of the ictal spike fell within the convex hull of the peri-ictal unit's spikes in principal component space. Further, a match confidence score from 0 to 1 was assigned to each matched ictal spike. For each peri-ictal unit, a Gaussian curve was fit to the distribution of voltages at each sampling point, then rescaled to a maximum height of one. Then, for each ictal spike matched to that unit, the spike's voltages were mapped to a point on each Gaussian and the average of these values over each sampling point resulted in the match confidence score.

We used probabilistic multi-unit firing rates based on putative neurons recorded by Utah microelectrode array.[54] The instantaneous probabilistic firing rate was calculated by convolving a discrete Gaussian kernel of standard deviation of 200 ms with the detected spike train, where each detection is scaled to its match confidence. Therefore, the probabilistic firing rate could not be artificially increased by an increase in background noise or by a single spike waveform matching with multiple putative units. The average probabilistic firing rate over a period of time was calculated by dividing the sum of all match confidence scores for detected units in that period by the length of the period. This average firing rate was used to quantify multi-unit activity in the pre-ictal (20 s before onset to seizure onset), pre-generalization (seizure onset to behavioural generalization) and post-generalization (behavioural generalization to seizure offset) periods. In addition, for each putative single unit, spike times of waveforms with >50% match confidence were displayed across the seizure epoch in a raster plot. Units were ranked for display based on overall firing rate during the seizure epoch. Code for firing rate calculation and raster plots can be found at https://github.com/edmerix/NeuroClass.

Additionally, to compare local neuronal firing in the Utah array region with global dynamics during seizure, the PLHG metric was computed on both macro- and microelectrodes for these subjects as before. After removing faulty electrodes and those near lobar/SOZ boundaries, macroelectrodes were partitioned by region into frontal, temporal, parietal and SOZ groups, along with a single electrode nearest the Utah array. Mean PLHG values over the seizure epoch were then calculated for each electrode group, including the group of Utah array microelectrodes.

Data availability

Data supporting the findings of this study are available from the corresponding author upon reasonable request. Data from iEEG.org and the EED are available online.

Results

Markers of LOC distinguish FBTC from FIA

Behavioural assessment of 42 FIA where video was available (from UWHC and Mayo Clinic) revealed verbal unresponsiveness in 80% of tested seizures, motor unresponsiveness in 79% and amnesia of seizure events in 84%. In 46% of tested FIA, patients failed to interact with examiner in any way (CSS 3) and in 79% they were not aware of having a seizure during the event (CSS 4).

Splitting LOC scoring in two equal halves in FIA (30 ± 18 s) revealed signs of a progression across time. Specifically, while 73% patients were not aware of having a seizure in the first half of FIA, this significantly increased to 97% in the second half (Fisher's exact test: $P = 0.007$). Verbal unresponsiveness, motor unresponsiveness and interaction with examiner also seemed to become more impaired in the second half (from 68 to 70%, from 54 to 74% and from 45 to 50%, respectively), but these variables did not reach statistical significance.

In the 25 FBTC for which the behaviour before generalization could be scored (duration of pre-generalization phase: 58 ± 67 s), pre-generalization behaviour was characterized by verbal unresponsiveness in 89% and motor unresponsiveness in 93%. Interaction with examiner was impaired in 90% (CSS 3) and patients were not aware of having a seizure (CSS 4) in 91% of seizures. Contrasting these outcomes with the first half of FIA, we found significantly more patients with motor unresponsiveness ($P = 0.01$; Fisher) and impaired interaction with examiner ($P = 0.001$; Fisher).

During FBTC seizures with pre-generalization phase lasting <60 s, LOC was found to be complete (impairment in all CSS items) in 16/19 of seizures, and incomplete (impairment in some but not all CSS items) in 3/19 seizures. Among the four FBTC seizures with a pre-generalization phase lasting >60 s and where CSS scoring could be reliably performed close to seizure onset, consciousness was preserved (all CSS scores preserved) in 4/4 seizures during the first half of pre-generalization phase and then full LOC occurred in 4/4 seizures during the second half of the pre-generalization phase. During the post-generalization ictal period, all FBTC were unresponsive and unable to sustain any interaction. At the group level, the occurrence of full unresponsiveness and inability to sustain any interaction was significantly more frequent during the post-generalization phase of FBTC than during the second half of FIA (respectively $P = 0.008$ and $P < 0.001$; Fisher).

SWA and B/D patterns differ between FIA and FBTC

The linear mixed-effects model for SWA revealed no initial change from baseline during the first half of FIA (Fig. 2 left panel; see

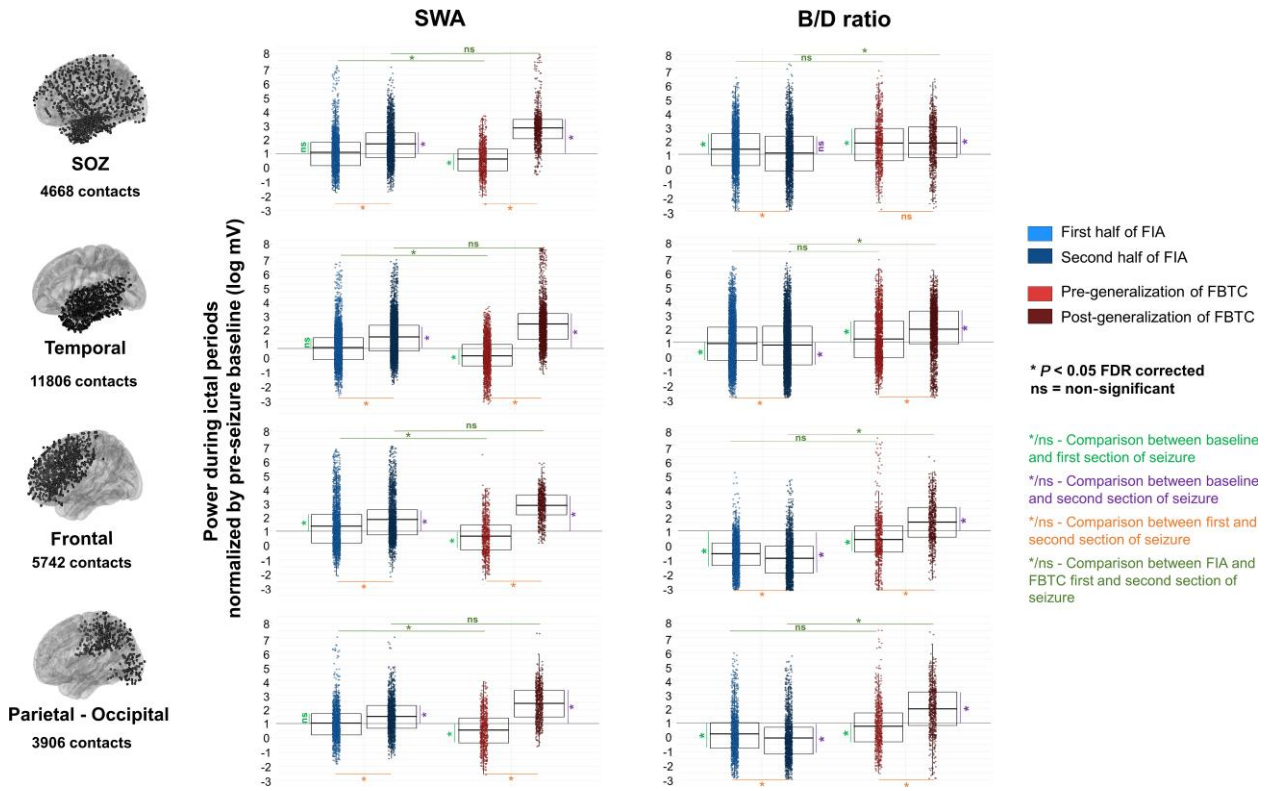

Figure 2 Group results for SWA power and B/D during both FIA and FBTC split by brain region (SOZ, temporal, frontal and parieto-occipital) and ictal period (first and second half of FIA, pre- and post-generalization of FBTC). Each dot represents the log of normalized power value (normalized by baseline activity) for an electrode contact. Results are shown for the first and second ictal period of FIA, and for the pre- and post-generalization period of FBTC seizures, respectively. Black horizontal lines indicate values of pre-ictal baseline activity. These results suggest that SWA increases and B/D decreases are prominent during the second ictal period during FIA. In contrast, SWA shows an overall decrease during the pre-generalization phase of FBTC, while it increases post-generalization. Similar patterns are observed for B/D ratio.

Supplementary Table 1A for all *Z* and *P*-values). A significant SWA power increase was subsequently seen in all brain areas during the second half (e.g. increase from 1.01 ± 0.03 to 1.67 ± 0.03 in SOZ; $Z = 22.89$, $P < 0.001$; Supplementary Tables 23A–B). In FBTC, a significant decrease of SWA compared to baseline was observed during pre-generalization ($P < 0.001$; see Supplementary Table 1A–B for all *Z* and *P* values), followed by increase in post-generalization in all brain areas (e.g. increase from 0.56 ± 0.03 to 2.64 ± 0.05 in SOZ; $Z = 50.1$, $P < 0.001$). While there were significantly less SWA in pre-generalization of FBTC than in the first half of FIA seizures ($P < 0.001$), there was no significant difference between post-generalization of FBTC compared to the second half of FIA.

During the first half of FIA, B/D decreased in all brain regions compared to baseline except in SOZ, where it was increased (Fig. 2 right panel; see Supplementary Table 2A–B for all *Z* and *P* values). A significant B/D decrease was further seen between first and second half of FIA in all brain areas (e.g. -0.16 ± 0.05 in parieto-occipital areas, $P < 0.001$; -0.93 ± 0.03 in frontal areas, $P < 0.001$; Supplementary Tables 24A–B). During the pre-generalization phase of FBTC (all 25 seizures together), B/D increased in SOZ and temporal regions but decreased in frontal and parieto-occipital regions. After generalization, B/D then remained elevated in SOZ while it sharply increased in all other brain regions. Between-seizure contrasts comparing the first half of FIA versus pre-generalization of FBTC were not significant, while decrease in B/D in all brain regions was found in the second half of FIA versus increase in B/D in post-generalization FBTC. Group analyses pooling all electrodes belonging to a single brain region within each subject led to similar results (see Supplementary Fig. 1 and Supplementary Tables 13–16). Group analysis comparing first and second halves of FIA and FBTC seizures can be found in the Supplementary Materials (Supplementary Fig. 2 and Supplementary Tables 17–18).

Secondary generalization during FBTC is accompanied by higher HG activity and cross-frequency coupling in many cortical areas

HG power showed an increase (<2-fold) as compared to baseline during first half of FIA in SOZ, temporal and parieto-occipital areas and remained elevated during the second half of FIA (Fig. 3, left panel, and see Supplementary Tables 3A and 25A and B). In contrast, during the pre-generalization phase of FBTC, HG power showed a marked increase (close to 2-fold as compared to baseline) in SOZ, temporal and parieto-occipital areas, which then further increased to >3-fold from baseline in all areas after generalization ($P < 0.001$). Between-seizure contrasts revealed no significant difference between the first half of FIA and the pre-generalization phase of FBTC, while significantly higher HG power was seen in post-generalization phase of FBTC compared to the second half of FIA (Supplementary Table 3B).

During the first half of FIA, PLHG increased from baseline in SOZ and temporal areas ($P < 0.001$; Fig. 3, right panel, and Supplementary Tables 4A and 26A) while it decreased in frontal and parieto-occipital areas ($P < 0.001$). During the second half, PLHG continued to show a

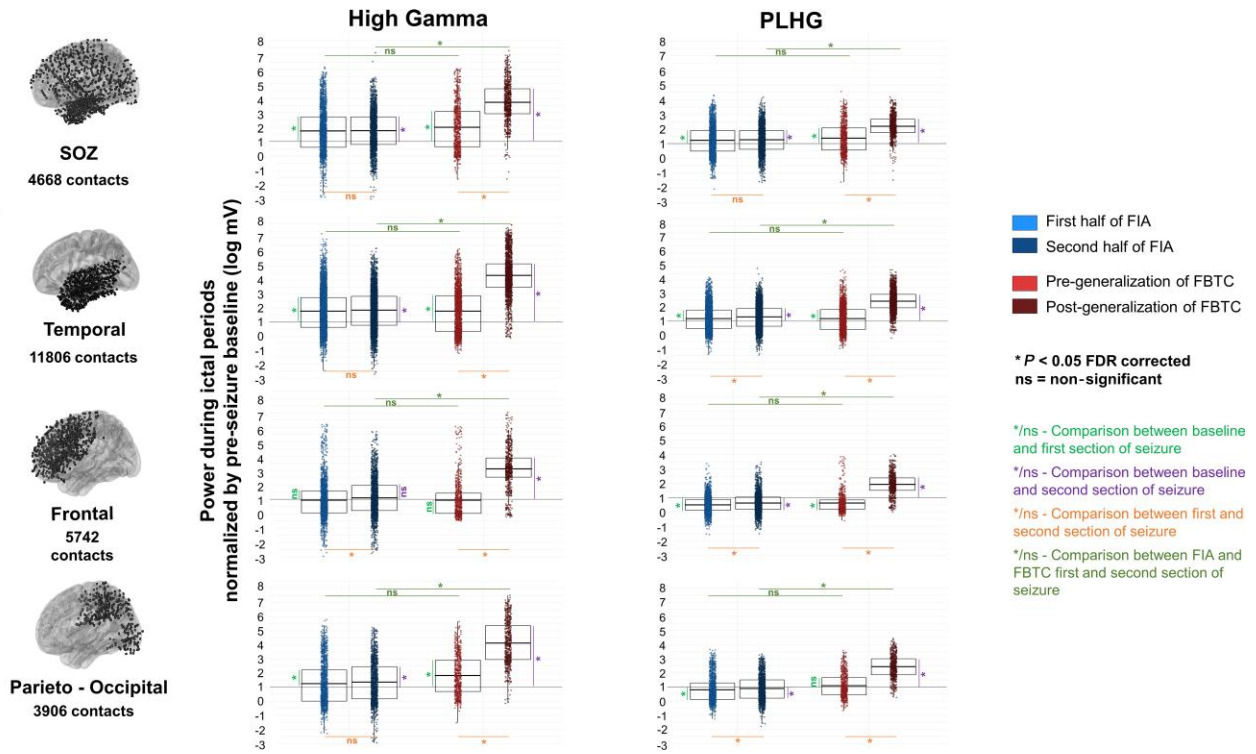

Figure 3 Group results for HG power and PLHG during both FIA and FBTC, split by brain region (SOZ, temporal, frontal and parieto-occipital) and ictal period (first and second half of FIA, pre- and post-generalization of FBTC). Each dot represents the log of normalized power value (normalized by baseline activity) for an electrode contact. Results were shown for the first and second ictal period of FIA, and for the pre- and post-generalization period of FBTC seizures, respectively. Black horizontal lines indicate values of pre-ictal baseline activity. These results suggest that HG and PLHG increase in SOZ and temporal lobe but decreases in the rest of the brain during FIA. In contrast, both HG and PLHG diffusely increase starting at the onset of FBTC, and further build up as FBTC progress. HG and PLHG were significantly higher during FBTC than during FIA for all brain areas and all ictal periods.

mild increase compared to baseline in temporal areas, remained decreased in frontal and parieto-occipital areas, and was more variable in the SOZ (1.35 ± 0.02, $P < 0.001$ for SOZ, 1.30 ± 0.01, $P < 0.001$ for temporal, 0.60 ± 0.01, $P < 0.001$ for frontal and 0.86 ± 0.02, $P = 0.024$ for parieto-occipital; Supplementary Table 26B). In contrast, during the pre-generalization phase of FBTC, PLHG increased nearly two times from baseline for all brain areas (Supplementary Table 26B). During the post-generalization phase, PLHG was further increased ($P < 0.001$ for all brain areas when comparing to baseline values, e.g. 2.41-fold increase in the parieto-occipital area; Supplementary Table 26B). Between-seizure contrasts revealed no significant difference between the first half of FIA and pre-generalization of FBTC, but significantly higher PLHG during the post-generalization phase of FBTC compared to the second half of FIA (Supplementary Table 4B). Group analyses pooling all electrodes belonging to a single brain region within each subject led to similar results (see Supplementary Fig. 1). Group analysis comparing first and second halves of FIA and FBTC seizures can be found in the Supplementary material (Supplementary Fig. 3 and Supplementary Tables 19–20).

Widespread but asynchronous ictal recruitment during FBTC

The ER analysis also showed that more channels were recruited in the ictal process during FBTC compared to FIA (69 ± 4 and $45 \pm 6\%$, respectively, $P < 0.001$; Supplementary Table 5; see also Supplementary Table 7 for pre- and post-generalization of FBTC versus FIA comparisons. Overall, channels that least frequently passed ER during FIA were located in the parietal lobe (29 versus 39–60% in other lobes, $P < 0.001$; Supplementary Table 6) and during FBTC, in the limbic network (58 versus 62–78% in other lobes, $P < 0.01$).

The analysis of the timing of ER threshold crossing revealed that the recruitment of channels into the ictal process was asynchronous both during FIA [example in Fig. 4A(i)] and FBTC [example in Fig. 4A(ii)]. Interestingly, we found that while more channels were recruited during FBTC, significantly more clusters of channels were also recruited more asynchronously (with a higher proportion of channels crossing ER threshold >1 s apart: $23 \pm 13\%$ in FBTC versus $10 \pm 7\%$ in FIA, $P < 0.001$; Supplementary Table 5).

To compare differences in synchrony of ictal patterns during FIA versus FBTC, we examined the dynamics of time-frequency activity across channels (Fig. 4B). During both seizure types, we observed asynchronous increases in SWA power across different channels, with most channels presenting SWA power peak towards the end of the seizure (during the second half of FIA or during the post-generalization phase of FBTC seizures). SWA power peaks were more asynchronous during FBTC than during FIA (34 ± 16 and $28 \pm 16\%$, $P = 0.025$; Supplementary Table 5). Similar to SWA, the timing of the most negative amplitude of individually detected SW most often occurred during the second half of the seizures (mean time of 75 ± 12 s for FBTC, and 63 ± 17 for FIA). The timing of occurrence of the most negative SW amplitude was again more asynchronous during FBTC as compared to FIA (42 ± 18 versus $35 \pm 16\%$ of SW amplitude peaks crossing threshold >1 s apart, $P = 0.012$; Supplementary Table 5).

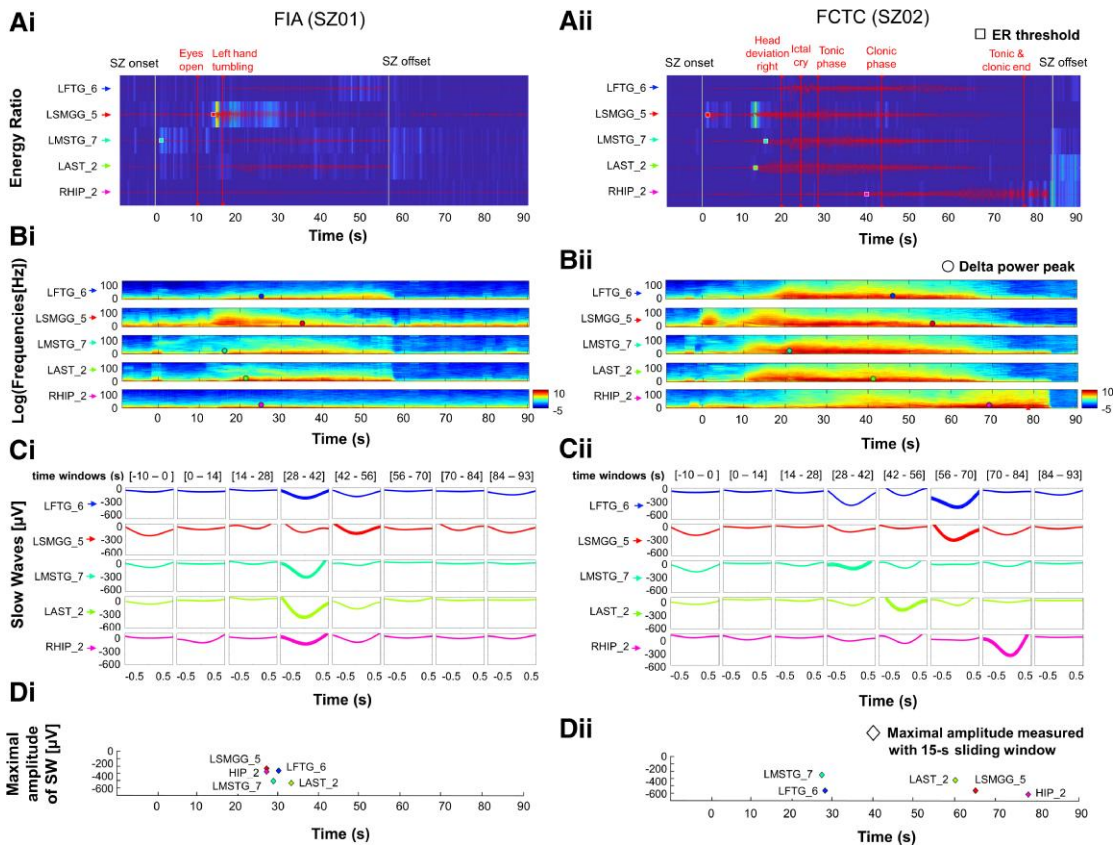

Figure 4 Asynchrony of channel recruitment, SWA power and SW amplitude peaks during FIA versus FBTC seizures. [**A**(**i** and **ii**)] Five representative channels are displayed for the same representative FIA and the FBTC seizures used in Fig. 1 above. The time points at which the ER threshold was exceeded are represented by filled squares for each channel. Channels were recruited asynchronously in both cases, but with fewer channels recruited during FIA than during FBTC. At the time of the behavioural generalization (start of the tonic phase marked with vertical line), only partial recruitment could be observed. Vertical lines mark behavioural events. [**B**(**i** and **ii**)] The peaks of SWA (delta) power are marked with filled circles on time-frequency plots for each representative channel, and revealed asynchronous for both FIA and FBTC seizures (see Supplementary Fig. 4 for the timing of HG power peaks for comparison). [**C**(**i** and **ii**)] SWs averaged for specific time intervals are highlighted in bold to mark maximal SW amplitude for each representative channel. [**D**(**i** and **ii**)] The timing of negative SW amplitude peaks are marked with filled diamonds for each representative channel. Note that the timing of occurrence of SW amplitude peaks is especially asynchronous during FBTC.

In contrast, during both seizure types we observed synchrony of HG power peaks across channels (Supplementary Fig. 4), which was specifically prominent during FBTC. Interestingly, during FBTC HG power also increased across the ictal period in channels that were not recruited by the seizure (did not pass the ER threshold; Supplementary Tables 27A–C and Supplementary Fig. 5).

A whole-brain increase in HG coincides with behavioural generalization

The previously mentioned group analysis performed on all seizures suggested a widespread increase in HG power and PLHG during FBTC compared to FIA, which built up from the first to the second half of the seizures. To further characterize whether such a late build-up in high-frequency activity was related to the occurrence of behavioural generalization itself, we examined the correspondence between spectral power time courses and ictal behaviour. During FIA, a minimal increase in HG power could be seen in the SOZ, peaking in the middle of the seizure (example in Fig. 5, right panel). During FBTC, stronger increases in HG power and PLHG were consistently seen in the SOZ from the seizure onset (see the example in Fig. 5, left panel), which further spread to all channels, with the sharpest slope for a whole-brain increase closely matching the time of behavioural generalization onset (see the example in Fig. 5B). Proof-of-principle analyses of the 20 FBTC with behavioural scoring showed that there was a significantly higher time concordance between the point with maximum slope of HG increase and behavioural generalization (10 ± 5.9 s from behavioural generalization; Supplementary Table 8) compared to seizure onset or offset. Interestingly, the temporal concordance with behavioural generalization was higher with PLHG (39.8 ± 9.83 s; Supplementary Table 8) than for the line length of HG (15 ± 6 s; Supplementary Table 8).

Increase in HG is not a muscular artefact

A linear regression between EMG and iEEG channels revealed that EMG accounted for only on average 1.31±0.34% (range 0.01–12%) of explained variance in the iEEG across the whole ictal period (Supplementary Fig. 6A and Supplementary Tables 21 and 22). In contrast, iEEG channels on average showed a shared variance of 43 ± 4% (range 12–91%). In fact, iEEG channels shared significantly higher variance after generalization than before generalization or during baseline compared to iEEG versus EMG [$t(19) = 3.69$, $P = 0.002$ for baseline; $t(19) = 9.4$, $P < 0.001$ for pre-generalization; $t(19) = 10.71$, $P < 0.001$ for post-generalization]. This suggests a minimal or non-existent contribution of muscle activity. Linear regression between deep versus superficial contacts revealed higher synchrony between deep contacts (amygdala, hippocampus) than between superficial contacts, especially during the post-generalization period (49 ± 7 then

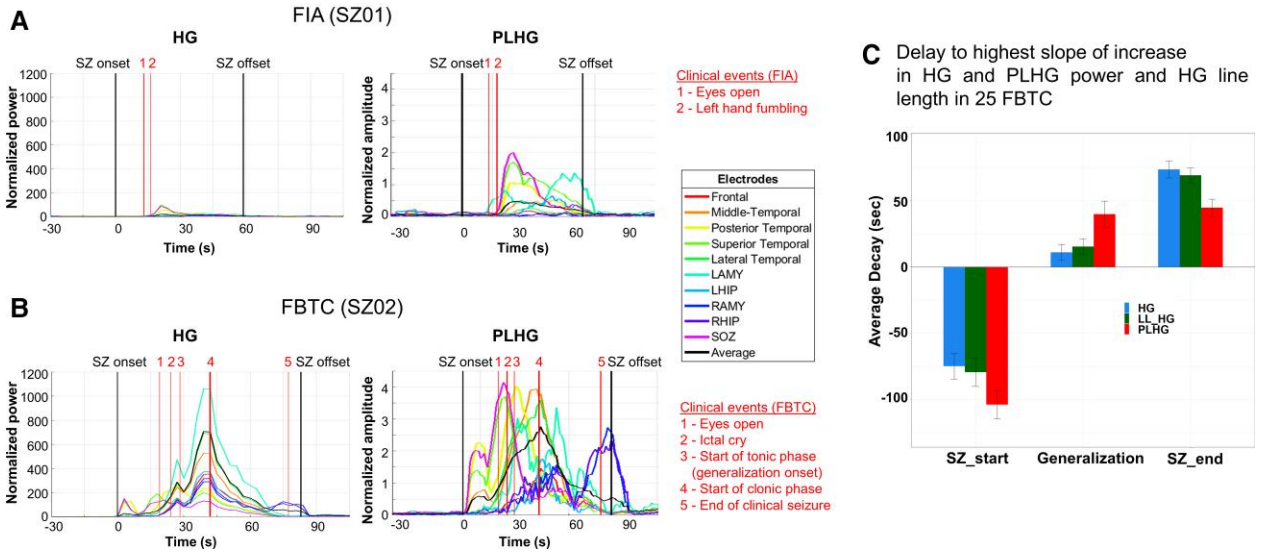

Figure 5 Temporal evolution of high-frequency rhythms (HG and PLHG) in two exemplar FBTC and FIA from the same patient as shown in Fig. 1 displayed along relevant behavioural events. (**A**) FIA. In FBTC (**B**), the widespread increase in HG and PLHG peaking at the generalization point (event 3) can be clearly seen. (**C**) The group results (from 25 FBTC) for the average delay between seizure start, generalization point and seizure end to the highest slope increase in HG power and PLHG.

61 ± 5% for superficial contacts, 65 ± 8 then 78 ± 5% for deep contacts; Supplementary Fig. 6B and Supplementary Table 21).

Increased neuronal firing rates accompany HG increases in non-SOZ areas during FBTC

To obtain a direct demonstration of the neuronal basis for high-frequency signal changes during FBTC, we used simultaneous iEEG and single-unit recordings in three FBTC recorded with Utah microelectrode arrays in areas located in the ictal penumbra (>2 cm from the SOZ) (see Supplementary Fig. 7). Before generalization time, probabilistic multi-unit firing rate changes compared to baseline were variable: the average increased in one FBTC and decreased in two others (+51.5, –43.4 and –48.5% change, respectively). In contrast, probabilistic multi-unit firing rates showed a sustained and consistent increase after the point of behavioural generalization compared to baseline (+215.8, +83.4 and +234.6% change, respectively). Increases in firing rates at generalization onset were accompanied by increases in HG within the whole brain (as observed in the other FBTC studied).

These unit firing rate increases occur alongside PLHG increases both in the iEEG channels close to the Utah array and in Utah array microelectrode channels (see Fig. 6). Multi-unit activity and PLHG appeared linked, except during brief peaks of multi-unit firing that do not show corresponding peaks of PLHG. This is sensible, as PLHG is predicted to especially increase due to highly synchronous firing, but not all firing.[42] Therefore, PLHG may not track multi-unit firing when firing is asynchronous, or when highly synchronous firing increases in frequency without increasing synchrony. Nevertheless, the tendency of these values to match over sustained periods supports the hypothesis that widespread PLHG increases are neuronal in origin.

Early LOC during FBTC pre-generalization phase is accompanied by decreased SWA and increased HG activity

To avoid confounds due to behavioural generalization when comparing signatures of LOC during FIA versus FBTC, we compared brain activity patterns during the whole FIA period to pre-generalization periods in FBTC seizures with early complete LOC (16/25 FBTC) and in FBTC seizures with preserved consciousness at onset followed by late LOC (4/25 FBTC). Compared to baseline, the whole FIA period was characterized by SWA increases in SOZ, temporal and frontal cortex ($P < 0.001$). In contrast, during the pre-generalization phase of FBTC with early LOC, we observed consistent decreases in SWA compared to baseline (Fig. 7A and Supplementary Table 9A). Between-group analysis revealed that SWA was indeed significantly lower during FBTC pre-generalization phase with early LOC compared to FIA in all brain areas ($P < 0.001$; see Supplementary Table 9B), while it was significantly higher during FBTC post-generalization ($P < 0.001$). When patients remained conscious during the first part of pre-generalization phase, SWA decreased as compared to baseline in fronto-temporal areas ($P < 0.001$) but not in parieto-occipital cortex. When LOC occurred during the second half of pre-generalization, SWA increased further as compared to baseline in parieto-occipital cortex ($P = 0.01$), but did not in SOZ, frontal and temporal regions.

HG power increased during FIA as compared to baseline in temporal lobe ($P < 0.001$; see Supplementary Table 11A), but not significantly in other areas. During the pre-generalization phase of FBTC with early LOC, HG power significantly increased in SOZ, temporal and parieto-occipital areas ($P < 0.001$; Fig. 7B), but not in frontal cortex. When patients remained conscious during the first part of the pre-generalization phase, HG did not increase compared to baseline in parieto-occipital areas, and even decreased compared to baseline in frontal and temporal areas ($P < 0.001$). When patients lost consciousness during the second half of pre-generalization phase, increased HG power was observed compared to baseline in SOZ, temporal and parieto-occipital cortex ($P < 0.001$), but not in frontal cortex. Post-generalization, increased HG power compared to baseline persisted in all previously mentioned brain areas and also increased in frontal cortex ($P < 0.001$), across all FBTC types. B/D and PLHG showed similar patterns of increases compared to both baseline and FIA during LOC in the pre-generalization phase,

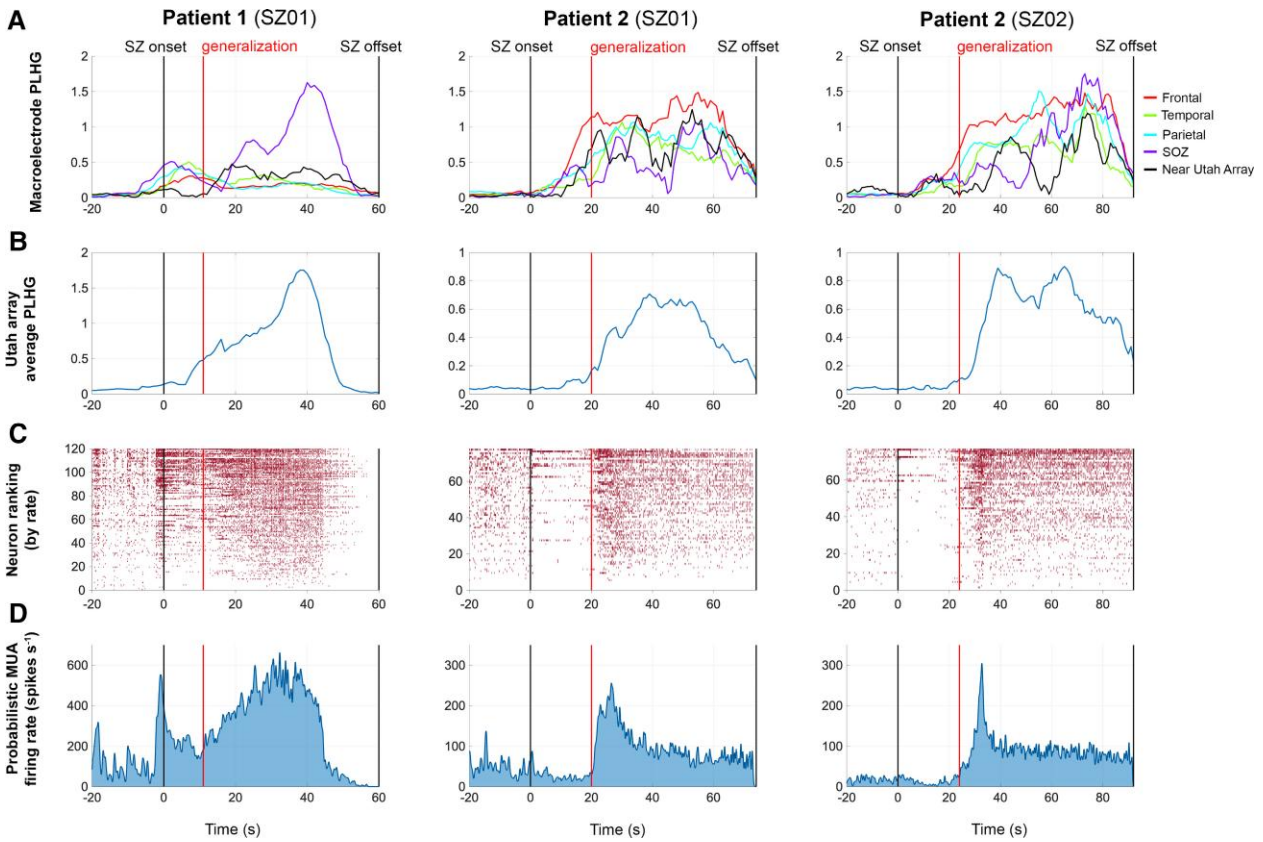

Figure 6 Temporal evolution of PLHG and neuronal firing during three FBTC from two patients implanted with Utah microelectrode arrays in areas remote from the SOZ. (**A**) PLHG for macroelectrodes in various locations across the brain. PLHG values in the SOZ and near the Utah array come from single distinct contacts, while PLHG values from frontal, temporal and parietal areas were averaged over several contacts in the corresponding lobe (see Supplementary Fig. 3). (**B**) Average PLHG calculated across all good Utah array channels. (**C**) Raster plot of single-unit firing times ordered by firing rate. Only spikes with match confidence of 50% or higher are plotted. (**D**) Probabilistic firing rate for the population were calculated over the seizure epoch. These results show similar high-frequency increase at the macro level—with increased PLHG—and at the micro level—with increased neuronal firing—and this both for ictal onset and behavioural generalization.

but with less consistency across subjects and seizure phases (see Supplementary Fig. 8 and Supplementary Tables 10 and 12).

Discussion

We found that unlike during FIA, the temporal evolution of FBTC is accompanied by a diffuse increase in markers of cortical activation (B/D, HG, PLHG) and ictal recruitment (number of channels crossing ictal ER threshold). Specifically, a whole-brain increase in HG power accompanied behavioural generalization onset, which was most synchronous in deep iEEG channels, could not be accounted for by EMG and was accompanied by increased multi-unit firing rates in areas remote from SOZ. Additionally, early LOC during FBTC was accompanied by decreased SWA and increased HG compared to baseline; HG increases, rather than SWA changes, also signalled a later occurrence of LOC during the pre-generalization phase of FBTC. Overall, these findings suggest different mechanisms for LOC during FBTC compared to FIA, with an increase in cortical activation and ictal recruitment rather than sleep-like activities. Interestingly, the maximum synchrony in deep iEEG sources at the time of generalization (especially strong in amygdala) suggests the potential contribution of a subcortical source.

Our results confirm and extend in a larger dataset the previous observation of widespread increases in cortical SWA during FIA of temporal lobe onset.[14] During FIA, increased SWA in frontal regions was indeed sleep-like: it was accompanied by a decrease in B/D, which reliably differentiates physiological sleep from wakefulness in iEEG recordings.[40,41] During FBTC, in contrast, B/D increased across the whole brain. The finding of widespread cortical activation fits with previous studies using electroconvulsive therapy in humans and with animal models showing diffusely increased brain metabolism and fMRI BOLD signal during FBTC.[14,21,55] The fact that some individual channels showed B/D increases before they were actively recruited into ictal rhythms, and that this phenomenon occurs specifically in FBTC and not in FIA, suggest that increased beta-delta ratio may at least in part be related to the activation of a third driver source, potentially of subcortical origin. Furthermore, our synchrony analyses revealed that while SWA power developed asynchronously throughout seizures, HG was very synchronous, suggesting once again a possible subcortical main driver for whole-brain increases in high-frequency activity during FBTC.

We also found a more widespread ictal activation during FBTC than during FIA. Indeed, FIA displayed PLHG increases that were mostly restricted to SOZ, while PLHG decreased in extra-SOZ brain regions. Increased PLHG as a form of cross-frequency-coupling (CFC) has been described in other studies pertaining to SOZ localization, seizure progression and/or termination.[27,56,57] CFC to some degree can also be a property of healthy neocortex, and not a uniquely distinctive feature of LOC. However, in the present

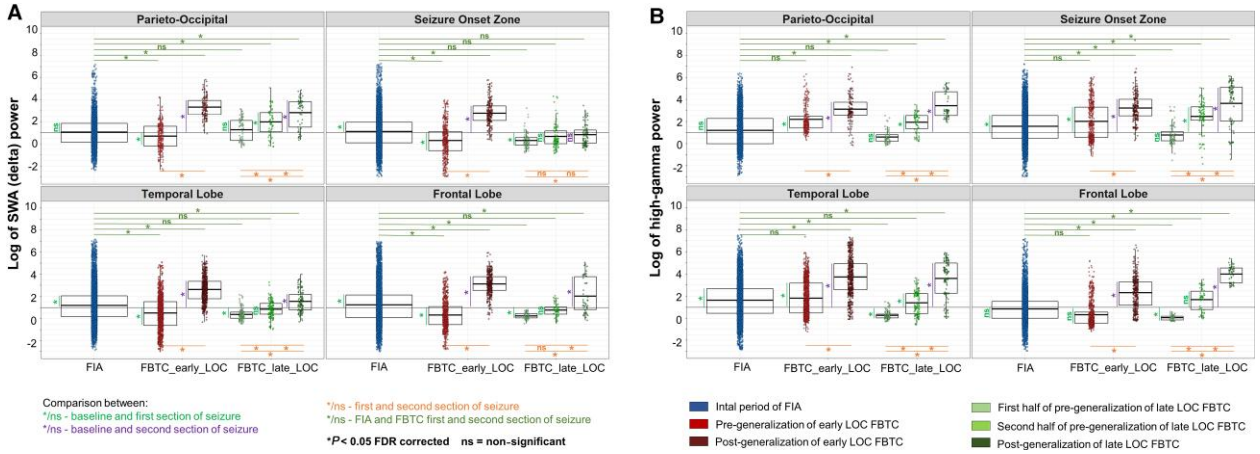

Figure 7 Group results for SWA and HG power during whole FIA ictal period compared to pre-generalization and post-generalization phases of FBTC with early versus late LOC. Each dot represents the log of normalized power value (normalized by baseline activity) for an electrode contact. Results are presented for the whole ictal period of FIA, pre- and post-generalization periods of FBTC with early LOC, and for the first and second ictal period of the pre-generalization phase and post-generalization phase for FBTC with late LOC, respectively. Black horizontal lines indicate values of pre-ictal baseline activity. These results suggest that while (**A**) LOC during FIA seizures is associated with widespread increases in SWA, (**B**) LOC during both the pre-generalization and the post-generalization phases of FBTC are accompanied by an increase in HG power, most consistently in posterior cortex: it is observed from seizure onset for FBTC with early LOC (while SWA is decreased compared to baseline); it is not observed during the first half, but occurs during the second half of pre-generalization in FBTC with late LOC, and persists in all seizures during pre-generalization phase where all patients show LOC.

context, increased PLHG suggests the presence of higher cortical activation during FBTC seizures compared to baseline, which became maximum in the post-generalization phase. In contrast, PLHG increased early and diffusely in the whole brain during FBTC and further built up with FBTC progression. Because PLHG increases reliably indicate areas that are recruited into ictal firing,[24,25] its progressive evolution during FBTC provides strong support for a more widespread ictal involvement than during FIA. Additionally, we found significantly more channels passing a validated ER threshold for ictal involvement during FBTC than during FIA. The higher cortical recruitment during FBTC, evidenced here using two independent quantitative markers of ictal recruitment, is in line with previous studies in smaller samples using less specific markers such as the visual detection of HFOs.[19] This finding may explain longer-lasting cognitive consequences of FBTC and through the induction of plastic changes, its association with poorer surgical outcomes. Interestingly, while more channels were recruited into the ictal process during FBTC than during FIA, we also found more asynchrony between clusters of channels. This was found using both the quantification of each channel's ictal onset by crossing of the ER threshold,[28] and the inspection of later ictal dynamics for SWA and SW amplitude peaks. This observation questions the fact that LOC during FBTC may be related to an increase in synchrony within cortical signals, as suggested in.[58] It also points to a possible association between the occurrence of FBTC and the development of multiple intracranial epileptic foci.[59] The tools developed in the present work may be used in future studies to assess whether the number of independent foci recruited during either FBTC and FIA differentially predicts multifocal seizures and poor surgical outcomes in individuals with epilepsy.

The electrophysiological hallmark of behavioural generalization was a widespread increase in HG power. This HG increase at generalization onset was especially synchronous in deeper channels (amygdala, and to a smaller extent, hippocampus). This suggests that deep sources particularly well-connected to limbic areas—such as arousal centres in the brainstem or basal forebrain—may be involved in spreading cortical activation during the generalization process. Unilateral blockade of inhibitory GABA neurotransmission in the basal forebrain is able to trigger bilateral limbic motor seizures in the rat.[60] The involvement of subcortical structures in seizure generalization is also supported by a previous single photon emission computed tomography (SPECT) study demonstrating increased cerebral blood flow in the brainstem and basal ganglia during FBTC compared to FIA.[55] This hypothesis is also in line with early work in cats suggesting that electrical activation of the brainstem can rapidly induce widespread increases in markers of cortical activation[61] while its ictal involvement can generate tonic posturing[62] and bilateral convulsions.[63] Another potential candidate for the subcortical mediation of seizure generalization might be the zona incerta. Indeed, rodent studies showed that high intensity cholinergic stimulation of the zona incerta leads to generalized seizures with the highest probability among all other subcortical sites.[64] The zona incerta[65] is a central relay of communication between the thalamus and the brainstem and presents especially rich interconnections with bilateral intralaminar and higher order nuclei of the thalamus.[65,66]

In the five patients where EMG channels were available, we found no meaningful contribution of EMG to HG signals, comparing EMG channels to deep and superficial channels from left as well as right hemispheres (average shared variance <5%). This finding suggests that as with the HG increase that is observed during FBTC postictal states,[48,49] the iEEG HG activity increases observed during and after generalization cannot be accounted for by increased EMG activity. Findings of higher synchrony in deep iEEG contacts, further away from the scalp and of only partial synchrony between cortical iEEG channels during the post-generalization phase also plead against an artefact as the primary source for the observed increases in HG signal.

To further ascertain of the neuronal origin of HG power increases, we quantified multi-unit activity data during three human FBTC. We found that increases in HG during FBTC were indeed

accompanied by sustained increases in neuronal firing even in areas remote from the SOZ. Taken together, these findings suggest that during FBTC—unlike during FIA—LOC is accompanied by widespread increases in neuronal activation throughout the brain. Of note, frequent FBTC recruiting a large number of areas may favour Hebbian plastic changes and secondary potentiation of multiple areas in the cortex, further favouring conditions for secondary epileptic foci to emerge, even in non-recruited brain areas. Such changes could explain worsened surgical outcomes and global cognitive impairment found in patients with frequent FBTC seizures.

Our behavioural results revealed that LOC was deeper during FBTC seizures compared to FIA seizures. Indeed, during most FIA, patients were not aware of having a seizure and were not responding to verbal and motor commands but could often still interact with the examiner in a minimal way. These results confirm previous reports showing a moderate consciousness impairment in FIA and a more complete one in FBTC.[10–12,33,67]

Interestingly, even during the pre-generalization phase of FBTC, responsiveness was more strongly impaired at the group level compared to during FIA, and about 2/3 of patients already displaying full LOC around seizure onset. Our analysis showed that during such an early LOC, SWA was paradoxically decreased compared to baseline, while HG was markedly increased especially in posterior cortex. During the subset of seizures where patients were conscious at seizure onset, and then become unconscious during second half of pre-generalization phase, the occurrence of increased HG power in posterior cortex also signalled the occurrence of LOC. Additionally, HG power remained elevated in the post-generalization phase, when all patients displayed LOC. BD and PLHG markers showed similar patterns, although being less consistent across FBTC seizures at the individual level. Overall, these results strongly suggest that unlike during FIA seizures where LOC is predicted by increased SWA, LOC during FBTC seizures is best predicted by increases in markers of cortical activation, specifically in parieto-occipital and temporal cortex. This prominent posterior involvement is in line with clinical and neuroimaging evidence[68] suggesting an important role of parieto-occipital cortex in human consciousness.

Of note, both FBTC and FIA were associated with increased SWA as the seizures evolved, which in FIA, was also accompanied by deeper LOC as the seizures progressed.[10,69] This finding is in line with recent studies suggesting a role of increased SWA in LOC during sleep.[70] However, increased SWA could not explain LOC occurring at an early stage during the pre-generalization phase of FBTC. Further studies should characterize similarities and differences between physiological and pathological SWA and its association with LOC during sleep and seizures.

This study has several important limitations. Only nine patients had both FBTC and FIA seizures. However, electrode coverage and demographics were similar between patients with FIA and FBTC at the group level, with broad electrode coverage and a large number of included seizures in both cases. Only three FBTC were recorded with multi-unit activity recordings, and the present findings should be confirmed in additional datasets with recordings within and outside the SOZ. Moreover, multi-unit activity recordings during FIA seizures would be a very interesting addition to the literature, but they were not readily available at the time the present manuscript was written. Finally, the evidence we have for subcortical third driver(s) is only indirect; animal studies may be more suited to test the contribution of various subcortical structures to seizure generalization and to explore various neuromodulation strategies. In combination with brain activity recordings, future studies should aim at probing behaviour throughout seizures with a faster temporal resolution, e.g. using the Automatic Responsiveness Testing in Epilepsy scale.[71] However, continuous behavioural sampling is extremely difficult to perform during FBTC. Retrospective collection of phenomenal experiences remembered by patient may provide useful complementary information about LOC in patients who are behaviourally unresponsive.[12]

Conclusion

In summary, our results show that FBTC are characterized by widespread increases in high-frequency activity and neuronal firing, which accompanies behavioural LOC and further progresses after onset of behavioural generalization. This high-frequency activity was most synchronous in deep iEEG channels, hinting to the possible contribution of subcortical drivers. These findings suggest that LOC during human FBTC may occur through a different mechanism than during FIA, with the presence of a widespread increase of neural activation throughout the cortex.

Acknowledgements

The authors would like to thank Pei-Ning Peggy Hsu for help with clinical information and William Marshall for statistical advice.

Funding

This work was supported by the Tiny Blue Dot Foundation (to M.B. and G.T.) and the Swiss National Science Foundation (SNF grants # 168437 and 177873 to E.J.). V.K. was partially funded by institutional resources of Czech Technical University in Prague.

Competing interests

The authors report no competing interests.

Supplementary material

Supplementary material is available at *Brain* online.

References

1. Zack MM, Kobau R. National and state estimates of the numbers of adults and children with active epilepsy—United States, 2015. *MMWR Morb Mortal Wkly Rep*. 2017;66:821–825.
2. Kalilani L, Sun X, Pelgrims B, Noack-Rink M, Villanueva V. The epidemiology of drug-resistant epilepsy: A systematic review and meta-analysis. *Epilepsia*. 2018;59:2179–2193.
3. Téllez-Zenteno JF, Dhar R, Wiebe S. Long-term seizure outcomes following epilepsy surgery: A systematic review and meta-analysis. *Brain*. 2005;128:1188–1198.
4. Cavanna AE, Monaco F. Brain mechanisms of altered conscious states during epileptic seizures. *Nat Rev Neurol*. 2009;5:267–276.
5. Blumenfeld H. Impaired consciousness in epilepsy. *Lancet Neurol*. 2012;11:814–826.
6. Nevalainen O, Ansakorpi H, Simola M, *et al*. Epilepsy-related clinical characteristics and mortality: A systematic review and meta-analysis. *Neurology*. 2014;83:1968–1977.

7. Devinsky O. Sudden, unexpected death in epilepsy. *N Engl J Med*. 2011;365:1801–1811.
8. Devinsky O, Hesdorffer DC, Thurman DJ, Lhatoo S, Richerson G. Sudden unexpected death in epilepsy: Epidemiology, mechanisms, and prevention. *Lancet Neurol*. 2016;15:1075–1088.
9. McPherson A, Rojas L, Bauerschmidt A, *et al*. Testing for minimal consciousness in complex partial and generalized tonic-clonic seizures. *Epilepsia*. 2012;53:e180–e183.
10. Yang L, Shklyar I, Lee HW, *et al*. Impaired consciousness in epilepsy investigated by a prospective responsiveness in epilepsy scale (RES). *Epilepsia*. 2012;53:437–447.
11. Johanson M, Valli K, Revonsuo A, Chaplin JE, Wedlund J-E. Alterations in the contents of consciousness in partial epileptic seizures. *Epilepsy Behav*. 2008;13:366–371.
12. Johanson M, Revonsuo A, Chaplin J, Wedlund J-E. Level and contents of consciousness in connection with partial epileptic seizures. *Epilepsy Behav*. 2003;4:279–285.
13. Shin JH, Joo EY, Seo D-W, Shon Y-M, Hong SB, Hong S-C. Prognostic factors determining poor postsurgical outcomes of mesial temporal lobe epilepsy. *PLoS ONE*. 2018;13:e0206095.
14. Englot DJ, Yang L, Hamid H, *et al*. Impaired consciousness in temporal lobe seizures: Role of cortical slow activity. *Brain*. 2010;133:3764–3777.
15. Kundishora AJ, Gummadavelli A, Ma C, *et al*. Restoring conscious arousal during focal limbic seizures with deep brain stimulation. *Cereb Cortex*. 2017;27:1964–1975.
16. Filipescu C, Lagarde S, Lambert I, *et al*. The effect of medial pulvinar stimulation on temporal lobe seizures. *Epilepsia*. 2019;60:e25–e30.
17. Yoo JY, Farooque P, Chen WC, *et al*. Ictal spread of medial temporal lobe seizures with and without secondary generalization: An intracranial electroencephalography analysis. *Epilepsia*. 2014;55:289–295.
18. Weiss SA, Banks GP, McKhann GM, *et al*. Ictal high frequency oscillations distinguish two types of seizure territories in humans. *Brain*. 2013;136:3796–3808.
19. Schönberger J, Birk N, Lachner-Piza D, Dümpelmann M, Schulze-Bonhage A, Jacobs J. High-frequency oscillations mirror severity of human temporal lobe seizures. *Ann Clin Transl Neurol*. 2019;6:2479–2488.
20. Schindler K, Leung H, Lehnertz K, Elger CE. How generalised are secondarily "generalised" tonic clonic seizures? *J Neurol Neurosurg Psychiatry*. 2007;78:993–996.
21. Blumenfeld H, Westerveld M, Ostroff RB, *et al*. Selective frontal, parietal, and temporal networks in generalized seizures. *Neuroimage*. 2003;19:1556–1566.
22. Bagshaw AP, Jacobs J, LeVan P, Dubeau F, Gotman J. Effect of sleep stage on interictal high-frequency oscillations recorded from depth macroelectrodes in patients with focal epilepsy. *Epilepsia*. 2009;50:617–628.
23. Smith EH, Merricks EM, Liou J-Y, *et al*. Dual mechanisms of ictal high frequency oscillations in human rhythmic onset seizures. *Sci Rep*. 2020;10:19166.
24. Schevon CA, Weiss SA, McKhann G, *et al*. Evidence of an inhibitory restraint of seizure activity in humans. *Nat Commun*. 2012;3:1060.
25. Smith EH, Liou J, Davis TS, *et al*. The ictal wavefront is the spatiotemporal source of discharges during spontaneous human seizures. *Nat Commun*. 2016;7:11098.
26. Schevon CA, Tobochnik S, Eissa T, *et al*. Multiscale recordings reveal the dynamic spatial structure of human seizures. *Neurobiol Dis*. 2019;127:303–311.
27. Weiss SA, Lemesiou A, Connors R, *et al*. Seizure localization using ictal phase-locked high gamma: A retrospective surgical outcome study. *Neurology*. 2015;84:2320–2328.
28. Bartolomei F, Chauvel P, Wendling F. Epileptogenicity of brain structures in human temporal lobe epilepsy: A quantified study from intracerebral EEG. *Brain*. 2008;131:1818–1830.
29. Bartolomei F, Cosandier-Rimele D, McGonigal A, *et al*. From mesial temporal lobe to temporoperisylvian seizures: A quantified study of temporal lobe seizure networks. *Epilepsia*. 2010;51:2147–2158.
30. Kini LG, Davis KA, Wagenaar JB. Data integration: Combined imaging and electrophysiology data in the cloud. *Neuroimage*. 2016;124:1175–1181.
31. Klatt J, Feldwisch-Drentrup H, Ihle M, *et al*. The EPILEPSIAE database: An extensive electroencephalography database of epilepsy patients. *Epilepsia*. 2012;53:1669–1676.
32. Fisher RS, Cross JH, D'Souza C, *et al*. Instruction manual for the ILAE 2017 operational classification of seizure types. *Epilepsia*. 2017;58:531–542.
33. Arthuis M, Valton L, Régis J, *et al*. Impaired consciousness during temporal lobe seizures is related to increased long-distance cortical-subcortical synchronization. *Brain*. 2009;132:2091–2101.
34. Blenkmann AO, Phillips HN, Princich JP, *et al*. Ielectrodes: A comprehensive open-source toolbox for depth and subdural grid electrode localization. *Front Neuroinformatics*. 2017;11:14.
35. Smith SM, Jenkinson M, Woolrich MW, *et al*. Advances in functional and structural MR image analysis and implementation as FSL. *Neuroimage*. 2004;23:S208–S219.
36. Lancaster JL, Woldorff MG, Parsons LM, *et al*. Automated Talairach atlas labels for functional brain mapping. *Hum Brain Mapp*. 2000;10:120–131.
37. Lancaster JL, Rainey LH, Summerlin JL, *et al*. Automated labeling of the human brain: A preliminary report on the development and evaluation of a forward-transform method. *Hum Brain Mapp*. 1997;5:238–242.
38. Lundstrom BN, Boly M, Duckrow R, Zaveri HP, Blumenfeld H. Slowing less than 1 Hz is decreased near the seizure onset zone. *Sci Rep*. 2019;9:6218.
39. Delorme A, Makeig S. EEGLAB: An open source toolbox for analysis of single-trial EEG dynamics including independent component analysis. *J Neurosci Methods*. 2004;134:9–21.
40. Kremen V, Brinkmann BH, Van Gompel JJ, Stead M, St Louis EK, Worrell GA. Automated unsupervised behavioral state classification using intracranial electrophysiology. *J Neural Eng*. 2019;16:026004.
41. Reed CM, Birch KG, Kamiński J, *et al*. Automatic detection of periods of slow wave sleep based on intracranial depth electrode recordings. *J Neurosci Methods*. 2017;282:1–8.
42. Eissa TL, Tryba AK, Marcuccilli CJ, *et al*. Multiscale aspects of generation of high-gamma activity during seizures in human neocortex. *Eneuro*. 2016;3:ENEURO.0141–15.2016.
43. Jirsch JD, Urrestarazu E, LeVan P, Olivier A, Dubeau F, Gotman J. High-frequency oscillations during human focal seizures. *Brain*. 2006;129:1593–1608.
44. Penny WD, Duzel E, Miller KJ, Ojemann JG. Testing for nested oscillation. *J Neurosci Methods*. 2008;174:50–61.
45. Benjamini Y, Hochberg Y. Controlling the false discovery rate: A practical and powerful approach to multiple testing. *J R Stat Soc Ser B Methodol*. 1995;57:289–300.
46. Bates D, Mächler M, Bolker B, Walker S. Fitting linear mixed-effects models using lme4. *J Stat Softw*. 2015;67:1–48.
47. Riedner BA, Vyazovskiy VV, Huber R, *et al*. Sleep homeostasis and cortical synchronization: III. A high-density EEG study of sleep slow waves in humans. *Sleep*. 2007;30:1643–1657.
48. Bateman LM, Schevon CA. Postictal clinical and EEG activity following intracranially recorded bilateral tonic-clonic seizures. *Epilepsia*. 2019;60:1746–1747.

49. Bateman LM, Mendiratta A, Liou J-Y, *et al*. Postictal clinical and electroencephalographic activity following intracranially recorded bilateral tonic-clonic seizures. *Epilepsia*. 2019;60:74–84.
50. McGonigal A, Marquis P, Medina S, *et al*. Postictal stereo-EEG changes following bilateral tonic-clonic seizures. *Epilepsia*. 2019;60:1743–1745.
51. Quiroga RQ, Nadasdy Z, Ben-Shaul Y. Unsupervised spike detection and sorting with wavelets and superparamagnetic clustering. *Neural Comput*. 2004;16:1661–1687.
52. Merricks EM, Smith EH, McKhann GM, *et al*. Single unit action potentials in humans and the effect of seizure activity. *Brain*. 2015;138:2891–2906.
53. Hill DN, Mehta SB, Kleinfeld D. Quality metrics to accompany spike sorting of extracellular signals. *J Neurosci*. 2011;31:8699–8705.
54. Merricks EM, Smith EH, Emerson RG, *et al*. Neuronal firing and waveform alterations through ictal recruitment in humans. *J Neurosci*. 2021;41:766–779.
55. Blumenfeld H, Varghese GI, Purcaro MJ, *et al*. Cortical and subcortical networks in human secondarily generalized tonic-clonic seizures. *Brain*. 2009;132:999–1012.
56. Palva JM, Palva S, Kaila K. Phase synchrony among neuronal oscillations in the human cortex. *J Neurosci*. 2005;25:3962–3972.
57. Canolty RT, Edwards E, Dalal SS, *et al*. High gamma power is phase-locked to theta oscillations in human neocortex. *Science*. 2006;313:1626–1628.
58. Bartolomei F, Wendling F, Régis J, Gavaret M, Guye M, Chauvel P. Pre-ictal synchronicity in limbic networks of mesial temporal lobe epilepsy. *Epilepsy Res*. 2004;61:89–104.
59. Tobochnik S, Bateman LM, Akman CI, *et al*. Tracking multisite seizure propagation using ictal high-gamma activity. *J Clin Neurophysiol*. 2021. Online ahead of print.
60. Gale K. Subcortical structures and pathways involved in convulsive seizure generation. *J Clin Neurophysiol*. 1992;9:264–277.
61. Moruzzi G, Magoun HW. Brain stem reticular formation and activation of the EEG. *Electroencephalogr Clin Neurophysiol*. 1949;1:455–473.
62. Browning RA. Role of the brain-stem reticular formation in tonic-clonic seizures: Lesion and pharmacological studies. *Fed Proc*. 1985;44:2425–2431.
63. Gastaut H, Naquet R, Fischerwilliams M. The pathophysiology of grand mal seizures generalized from the start. *J Nerv Ment Dis*. 1958;127:21–33.
64. Brudzynski SM, Cruickshank JW, McLachlan RS. Cholinergic mechanisms in generalized seizures: Importance of the zona incerta. *Can J Neurol Sci*. 1995;22:116–120.
65. Wang X, Chou X-L, Zhang LI, Tao HW. Zona incerta: An integrative node for global behavioral modulation. *Trends Neurosci*. 2020;43:82–87.
66. Power BD, Mitrofanis J. Zona incerta: substrate for contralateral interconnectivity in the thalamus of rats. *J Comp Neurol*. 2001;436:52–63.
67. Bauerschmidt A, Koshkelashvili N, Ezeani CC, *et al*. Prospective assessment of ictal behavior using the revised responsiveness in epilepsy scale (RES-II). *Epilepsy Behav*. 2013;26:25–28.
68. Boly M, Massimini M, Tsuchiya N, Postle BR, Koch C, Tononi G. Are the neural correlates of consciousness in the front or in the back of the cerebral cortex? Clinical and neuroimaging evidence. *J Neurosci*. 2017;37:9603–9613.
69. Jobst BC, Williamson PD, Neuschwander TB, Darcey TM, Thadani VM, Roberts DW. Secondarily generalized seizures in mesial temporal epilepsy: Clinical characteristics, lateralizing signs, and association with sleep-wake cycle. *Epilepsia*. 2001;42:1279–1287.
70. Siclari F, Baird B, Perogamvros L, *et al*. The neural correlates of dreaming. *Nat Neurosci*. 2017;20:872–878.
71. Touloumes G, Morse E, Chen WC, *et al*. Human bedside evaluation versus automatic responsiveness testing in epilepsy (ARTiE). *Epilepsia*. 2016;57:e28–e32.